

Pose Randomization for Weakly Paired Image Style Translation

Zexi Chen, Jiaxin Guo, Xuecheng Xu, Yunkai Wang, Yue Wang, Rong Xiong

Abstract—Utilizing the trained model under different conditions without data annotation is attractive for robot applications. Towards this goal, one class of methods is to translate the image style from the training environment to the current one. Conventional studies on image style translation mainly focus on two settings: paired data on images from two domains with exactly aligned content, and unpaired data, with independent content. In this paper, we would like to propose a new setting, where the content in the two images is aligned with error in poses. We consider that this setting is more practical since robots with various sensors are able to align the data up to some error level, even with different styles. To solve this problem, we propose PROGAN to learn a style translator by intentionally transforming the original domain images with a noisy pose, then matching the distribution of translated transformed images and the distribution of the target domain images. The adversarial training enforces the network to learn the style translation, avoiding being entangled with other variations. In addition, we propose two pose estimation based self-supervised tasks to further improve the performance. Finally, PROGAN is validated on both simulated and real-world collected data to show the effectiveness. Results on down-stream tasks, classification, road segmentation, object detection, and feature matching show its potential for real applications. Code is available here.

I. INTRODUCTION

Learning is essential to endowing the robots with high-level of understanding of the environment. Considering the environmental changes and various robotic configurations, we have to collect and annotate data for each robot under each environmental condition, in order to train a model with good performance. Even when we have the trained model, a new dataset should be built and annotated again and the model has to be further trained when a new condition occurs. As the annotation takes intensive labor and time, this workflow may not be acceptable in the real application. Therefore, the problem is how to adapt the model to the new condition.

Transfer learning is such a solution to improve the performance of the model trained in one condition, called the target domain, but tested in a new condition, called the original domain, with minimal human labor i.e. data annotation. A common setting in transfer learning is that, we have annotated supervised data in the target domain, and unannotated unsupervised data in the original domain, and we have a model trained with the annotated target domain data, but we would like to use it for prediction on the original domain data. This setting is very useful for robotic tasks,

Zexi Chen, Jiaxin Guo, Xuecheng Xu, Yunkai Wang, Yue Wang, Rong Xiong are with the State Key Laboratory of Industrial Control Technology and Institute of Cyber-Systems and Control, Zhejiang University, Zhejiang, China. Yue Wang is the corresponding author wangyue@iipc.zju.edu.cn.

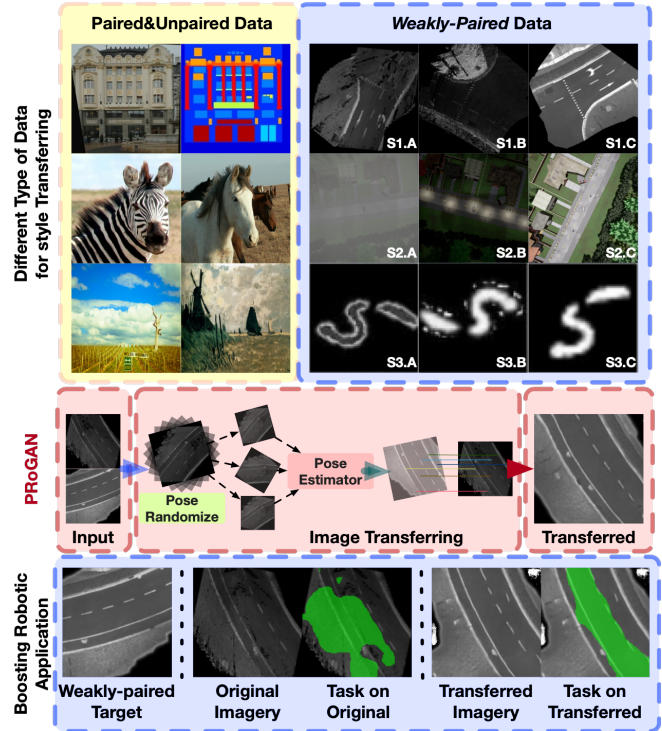


Fig. 1: **Top Left** is a combination of widely adopted paired&unpaired dataset for GANs' benchmarks. They are *Facades*, *Horse2Zebra* and *Monet2Photo* from top to bottom with a consensus that objects are upright in the gravity direction. **Top Right** is the weakly-paired dataset that we conduct our experiments on, and they are obtained from/by: *Aero-Ground*(S1), *WeakPair* dataset(S2, and transforming *MNIST*(S3). **Middle** shows how PROGAN deals with weakly-paired data. **Bottom Left**: Weakly paired images for the style transfer training. **Bottom Middle**: Original imagery and task on it. **Bottom Right**: Transferred imagery by PROGAN and correspondingly succeeded task.

such as transferring a detector trained in sunny data to rainy days.

A popular class of transfer learning methods is image style translation, which changes the style of an image, to another style without changing the content, thus a model learned in the target domain can be applied to images translated from the original domain. It has been applied in place recognition [21], vehicle detection [20] and semantic segmentation [7]. Currently, in this class, there are two typical tasks, paired image translation, and unpaired image translation. In the paired image translation, the contents for the two images from two domains are exactly the same. To deal with this task, PIX2PIX[12] proposes a generative adversarial network

(GAN) based solution and achieves good performance. However, in many applications, it is very difficult to obtain exactly paired data. Therefore, in the unpaired image translation, more than the style difference, the contents in the two images can be different. Aiming at this task, some methods are proposed [26, 4, 11]. The main idea of these works is to disentangle the content and style in the feature space, so that content and style features can be assembled. However, as this task has very limited supervision, the boundary between the learned content and style can be vague, probably leading to the failure of translation. We argue that in the robotic tasks, with all types of sensors, it is still hard to collect exactly paired data, but is possible to collect paired data with large overlap given reasonable error level, which we name as *weakly-paired* data. Given the definition of *weakly-paired* data, a style translator trained on it is a perfect match for boosting robotics tasks among different domains.

In this paper, we propose pose randomization GAN (PRoGAN) to solve weakly-paired image style translation. As shown in Fig. 2, the backbone of PRoGAN is GAN. According to [9], the equilibrium of GAN is a match between the distribution of the generated data and that of the target data. Therefore, we use GAN to match the distribution of target domain images, and that of original domain images warped with random poses, so that the network can be enforced to learn style translation without being entangled with pose transform, which is proposed as pose randomization. In addition, we also propose a self-supervision task by estimating the rotation among intermediate images, further constraining the content invariance during the style transfer. In the experiments, PRoGAN outperforms the unpaired data based methods on classification, segmentation, detection and feature points matching (Fig. 1). The contributions can be summarized as

- A new task is proposed as *weakly-paired image style translation*, which tolerates reasonable pose error injected in the conventional paired data task, thus making it much more practical for robotic applications.
- PRoGAN is proposed to solve the weakly-paired image style translation problem by intentionally matching the difference between the translated images and the original images induced by pose error, so that the content invariance can be better achieved.
- A self-supervision method is proposed to further improve the content invariance during the image translation by utilizing a pose estimator to find the relative pose between the randomized original images explicitly.
- A new weakly-paired dataset *WeakPair* [27] built in Carla [6] and real-world is released for research and this dataset supports the experiments of the proposed method, which demonstrates superior performance in 4 typical robotic tasks.

II. RELATED WORK

A. Image to image Translation

In computer vision, style translation problems are general tasks that aim to translate an input image from the original

domain to the target domain. GANs have achieved excellent results in translation, without any hand-crafted labels.

Many models have been proposed for translating paired images. Introduced by Zhu et al. [12], PIX2PIX is a classical framework for paired image-to-image translation, which utilizes condition GAN to learn a mapping representation from input to output images. Some other methods also tackle the unpaired image translation problems with the goal of translating images from the original domain to the target domain without any alignments. CYCLEGAN [26] utilizes a cycle framework, of which the cycle-consistency loss provides a regularization to prevent generators from excessive hallucinations and mode collapse. However, what it succeeds in are tasks involving color and texture changes, for tasks involved with geometric transformations and style translations, it starts to fail.

For these weakly paired images, UNIT [17] assumes a shared-latent space and proposes an unsupervised image-to-image translation framework based on Coupled GANs. STARGAN [4] is proposed to perform translations for multiple domains using only a single model, utilizing a mask vector method to control all available domain labels. UGATIT [14] incorporates a new attention module and AdaLIN for unsupervised translation. DRIT++ [16] is presented to generate diverse outputs without paired training images based on disentangled representation. MUNIT [11] assumes that the image representation can be decomposed into a content code that is domain-invariant, and a style code that captures domain-specific properties.

B. Self-supervised Learning

Self-supervised (SS) learning is a powerful approach for representation learning using unlabeled data. SS generally involves learning from tasks designed to resemble supervised learning in the way that "labels" can be created from the data itself without human labor [5]. [8] utilizes input image rotations by four certain degrees and train the model with the 4-class classifier to recognize the four rotations. The pretext task offers a powerful supervisory signal for semantic feature learning. However, during a GAN training process, it is often unstable and easily forgets previous tasks when searching for a Nash equilibrium in a high-dimensional space. A number of approaches based on SS have been proven successful for GANs training. Tran et al. [24] aim to improve GANs by applying SS learning via the geometric transformation on input images and assign the pseudo-labels to these transformed images. Chen et al. propose the self-supervised GAN [1], adding auxiliary rotation loss as a self-supervised loss to the discriminator.

C. Domain Randomization

Domain randomization (DR) is a complementary class of methods for domain adaptation, aiming to randomize parts of the domain to which the model should not be sensitive. Tobin et al. [23] utilize DR for addressing the reality gap. They randomize the simulator to expose the model to different environments at training time. [25] is proposed to randomize

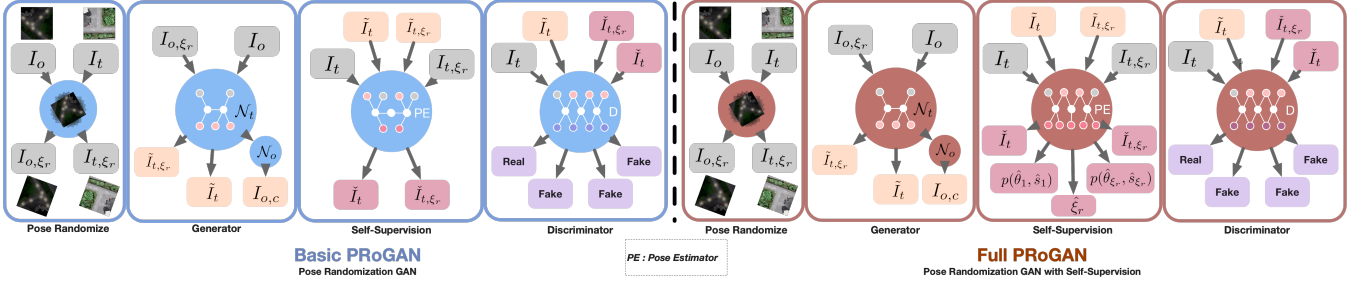


Fig. 2: The overview training structure of the PRoGAN. The goal is to transfer the “original” image (I_o) from its own domain to the “target” domain. Two versions of PRoGAN are proposed in the form of “Basic” and “Full”. In each version of PRoGAN, training processes in the order of left to right.

the synthetic images with styles of real images in terms of visual appearance using auxiliary sim-to-real datasets.

III. PROGAN FOR WEAKLY-PAIRED DATA IMAGE STYLE TRANSLATION

A typical example for paired, unpaired and the proposed weakly paired data is shown in Fig. 1. One can see that for paired data, the two images with different style, have perfect aligned content. For the unpaired one, the two images are unrelated in data. For the *weakly-paired* data, the contents in the images are the same, but not aligned. We consider that such a setting is not trivial. Since robots carry multi-sensors to perceive geometric measurements, coarsely alignment of the images with different styles is reasonable.

We formally state the weakly-paired data image style translation as a generative process of target image I_t using the original image I_o :

$$I_t = T(f(I_o), \xi) \quad (1)$$

where f and T are style translation process, and the image geometric transformation process, ξ is the relative pose between the two images, which parameterizes T . Note that we keep image relative pose in $\text{SIM}(2)$

$$\xi = \begin{pmatrix} s\mathbf{R}_\theta & \mathbf{t} \\ 0 & 1 \end{pmatrix} \in \text{SIM}(2) \quad (2)$$

where $s \in \mathbb{R}^+$ is the scale, $\mathbf{R}_\theta \in \text{SO}(2)$ is the rotation matrix generated by the heading angle θ , and $\mathbf{t} \in \mathbb{R}^2$ is the displacement vector and that ξ in this problem remains unknown.

The aim of *weakly-paired* data style translation is to learn a network \mathcal{N}_t to approximate f from dataset $\{I_o, I_t\}$, so that original image can be translated using \mathcal{N}_t . The challenge of this problem is to keep the learned function \mathcal{N}_t only translating style while given no intermediate supervision. Simply learning a network \mathcal{N}_t between the two images obviously leads to a process entangled with style, pose and content. On the other hand, regarding the image pairs as an unpaired image does not utilize the information of bounded ξ , leaving a large improvement margin.

A. Pose Randomization

We propose ProGAN to learn \mathcal{N}_t based on the weakly paired data. The main idea to eliminate the entanglement is

to intentionally inject noisy relative pose p to original domain images $\{I_o\}$, so that the distribution of image difference between the noisy original domain and the target domain, is only induced by style change. Thus, we can learn \mathcal{N}_t to capture this process.

TRANSFORMED IMAGE DISTRIBUTION MATCH: Note that T and f are commutative, we have

$$I_t = f(T(I_o, \xi)) = f(I_{o,\xi}) \quad (3)$$

where $I_{o,\xi}$ is I_o transformed with ξ . Note that we do not really have such images as ξ for each pair is unknown. However, as we roughly know the distribution of ξ according to the robot sensors, we can randomize ξ with ξ_r to generate a set of $\{I_{o,\xi_r}\}$, leading to a distribution match of generated images and the real transformed images

$$p(I_{o,\xi}) \approx p(I_{o,\xi_r}) \quad (4)$$

where $p(\cdot)$ is the probability density of \cdot .

TARGET IMAGE DISTRIBUTION MATCH: We then apply a neural network \mathcal{N}_t to transfer the style of I_{o,ξ_r} to generate \tilde{I}_t

$$\tilde{I}_t = \mathcal{N}_t(I_{o,\xi_r}), \quad I_{o,\xi_r} \sim p(I_{o,\xi_r}) \quad (5)$$

Recalling (3), we can approximate the generative process of I_t with (5) in the sense of probability distribution.

Since GAN [9] provides a tool for matching the distribution of generated images and the target images, we utilize it to train the match of $p(\tilde{I}_t)$ and $p(I_t)$. Specifically, the discriminator loss \mathcal{L}_D is designed as

$$\mathcal{L}_D = P_{\tilde{I}_t}^F + P_{I_t}^T, \quad (6)$$

and the generator loss \mathcal{L}_G is designed as

$$\mathcal{L}_G = P_{\tilde{I}_t}^T, \quad (7)$$

where P^T and P^F stands for predicting \cdot to be true and false respectively.

RELATIVE POSE GENERATOR: Based on the GAN introduced above, \mathcal{N}_t is learned to approximate f to transfer the style of the image. We further design a solver to estimate the exact relative pose $\hat{\xi}$ between a pair of data. Therefore, we can follow (1) to first change the style as $\tilde{I}_t = f(I_o)$, then use the estimated $\hat{\xi}$ to generate the final \tilde{I}_t .

To estimate the relative pose $\hat{\xi}$, we leverage the deep phase correlation (DPC)[2], which results in a distribution of relative rotation and scale changes $p(\hat{\xi}^{\hat{\theta}_1, \hat{s}_1})$ by

$$p(\hat{\xi}^{\hat{\theta}_1, \hat{s}_1}) = \mathfrak{C}(\mathfrak{L}(\mathfrak{F}(\tilde{I}_t)), \mathfrak{L}(\mathfrak{F}(I_t))) \quad (8)$$

where \mathfrak{F} is the discrete Fourier Transform, \mathfrak{L} is the log polar transform and \mathfrak{C} is the phase correlation solver. To make the solver differentiable, we use expectation as the estimation of $\hat{\xi}$. Thus the rotation $\hat{\theta}_1$ and scale \hat{s}_1 are

$$(\hat{\theta}_1, \hat{s}_1) = \mathbb{E}(p(\hat{\xi}^{\hat{\theta}_1, \hat{s}_1})), \quad (9)$$

$$\tilde{I}_t = \begin{bmatrix} \hat{s}_1 \mathbf{R}_{\hat{\theta}_1} & 0 \\ 0 & 1 \end{bmatrix} \tilde{I}_t \quad (10)$$

where $\mathbb{E}(\cdot)$ is the expectation of \cdot . We rotate and resize \tilde{I}_t referring to $\hat{\theta}_1$ and \hat{s}_1 with the result of \tilde{I}_t and calculate the relative displacement distribution $p(\hat{\xi}^{\hat{\theta}_1})$ between \tilde{I}_t and I_t :

$$p(\hat{\xi}^{\hat{\theta}_1}) = \mathfrak{C}(\tilde{I}_t, I_t), \quad (11)$$

$$\hat{t}_1 = \mathbb{E}(p(\hat{\xi}^{\hat{\theta}_1})). \quad (12)$$

Finally, we arrive at \tilde{I}_t by

$$\tilde{I}_t = \begin{bmatrix} 0 & \hat{t}_1 \\ 0 & 1 \end{bmatrix} \tilde{I}_t = \begin{bmatrix} \hat{s}_1 \mathbf{R}_{\hat{\theta}_1} & \hat{t}_1 \\ 0 & 1 \end{bmatrix} \tilde{I}_t. \quad (13)$$

By now, the generated image has the process

$$\tilde{I}_t = T(\mathcal{N}_t(I_o), \xi). \quad (14)$$

Obviously, \tilde{I}_t should be exactly the same with I_t . Moreover, we can also apply the same procedure to I_{o, ξ_r} to generate \tilde{I}_{t, ξ_r} , which should be the same to I_{t, ξ_r} . Therefore, following the one-to-one generated target image, we can design a pixel level loss terms as

$$\mathcal{L}_{trans} = \|I_t - \tilde{I}_t\|_1 + \|I_{t, \xi_r} - \tilde{I}_{t, \xi_r}\|_1, \quad (15)$$

where $\|\cdot\|_1$ is the L1 norm of \cdot .

JOINT LOSS AND TRAINING: Before introducing the loss function, one cyclic manner is adopted in the PRoGAN to avoid model collapse. An \mathcal{N}_o is leveraged to translate I_t back to a fake I_o . Now \tilde{I}_t will goes through \mathcal{N}_o after it got transformed from \mathcal{N}_t and becomes a $I_{o, c}$.

$$I_{o, c} = \mathcal{N}_o[\mathcal{N}_t(I_o)] \quad (16)$$

At this point, the **BASIC** version of PRoGAN is explicitly introduced and the losses in the training include one from the generator and another one from the discriminator. Losses \mathcal{L}_G calculated in the generator includes losses from CGAN in predicting the desired identity of \tilde{I}_t and \tilde{I}_t with respect to I_t , the enhanced L1 loss between the set \tilde{I}_t, I_t and $\tilde{I}_{t, \xi_r}, I_{t, \xi_r}$ and a cycle loss between $I_{o, c}$ and I_o :

$$\mathcal{L}_{cycle} = \|I_o - I_{o, c}\|_1, \quad (17)$$

$$\mathcal{L}_G = \mathcal{L}_{trans} + \mathcal{L}_{cycle} + P_{\tilde{I}_t}^T + P_{\tilde{I}_t}^T. \quad (18)$$

The discriminator loss is constructed by predicting the true identity of $\tilde{I}_t, \tilde{I}_t, \tilde{I}_{t, \xi_r}$ and I_t :

$$\mathcal{L}_D = P_{\tilde{I}_t}^F + P_{\tilde{I}_t}^F + P_{\tilde{I}_{t, \xi_r}}^F + P_{\tilde{I}_t}^T, \quad (19)$$

and the total loss \mathcal{L}_{All} is the sum of \mathcal{L}_G and \mathcal{L}_D :

$$\mathcal{L}_{PRoGAN_{BASIC}} = \mathcal{L}_G + \mathcal{L}_D \quad (20)$$

B. Self-supervision Tasks

During the training of PRoGAN, there are intermediate results whose relative poses are known, which can thus be utilized as a self-supervision to further constrain the network, improving the final performance.

RANDOMIZED POSE AS SELF-SUPERVISION: In pose randomization, we intentionally inject the noisy pose ξ_r to transform the images. This pose is exactly known, and can be utilized as a self-supervision. As mentioned in (14), we have \tilde{I}_t and \tilde{I}_{t, ξ_r} generated by N_t and T . Their relative angle is ξ_r . Motivated by this equality, we apply the DPC in (10) and (13) to \tilde{I}_t and \tilde{I}_{t, ξ_r} , resulting in the distribution of $p(\hat{\xi}_r)$, which is supervised by the KLD between the one-hot distribution centering at ξ_r

$$\mathcal{L}_{\xi_r} = KLD(p(\hat{\xi}_r), \mathbf{1}_{\xi_r}) \quad (21)$$

where $\mathbf{1}$ indicates for the one-hot distribution centering at \cdot . For implementation, we only use the first stage of DPC to estimate rotation, upon which the loss term is built for simplicity.

RELATIVE POSE EQUALITY AS SELF-SUPERVISION: Another supervision is built between the relative pose estimation from (I_t, \tilde{I}_t) , and $(I_{t, \xi_r}, \tilde{I}_{t, \xi_r})$. Note that only the rotation part of the two estimation result should be equal. The translation part is affected by the noisy pose ξ_r . Therefore, we use the intermediate DPC output of $p(\hat{\theta}_1, \hat{s}_1)$ as in (10), and $p(\hat{\theta}_{\xi_r}, \hat{s}_{\xi_r})$, to measure their similarity, leading to a KLD based loss term as

$$\mathcal{L}_{\theta, s} = KLD[p(\hat{\theta}_1, \hat{s}_1), p(\hat{\theta}_{\xi_r}, \hat{s}_{\xi_r})] \quad (22)$$

With all the loss terms introduced above (20), (21) and (22), we finally present the joint loss as

$$\mathcal{L}_{PRoGAN_{FULL}} = \mathcal{L}_{PRoGAN_{BASIC}} + \mathcal{L}_{\theta, s} + \mathcal{L}_{\xi_r} \quad (23)$$

Upon which, we name the resultant network as **FULL** version of PRoGAN.

C. Implementation Details

To achieve high-resolution image translation, we adopt the network from [13], which contains Resnet blocks for generator network. To realize the classification for each patch, we adopt 70×70 PatchGAN [12] for the discriminator network, which has fewer parameters and can work on arbitrary size images. All networks are trained from scratch with batch normalization and the learning rate of 1.5×10^{-5} .

IV. EXPERIMENTS: DATASET AND SETUP

Our approach is evaluated on both simulation and real-world datasets including four different tasks. The simulation dataset is named *WeakPair* as one of the contributions of this paper and the real-world dataset is the *Aero-Ground* and the *MNIST*. Tasks including classification(CL), object detection(OD), feature matching(FM) and road segmentation(RS) are tested on the dataset(s) shown in TABLE I.

TABLE I: Indication of the certain dataset(s) that each task is tested on.

Dataset	Tasks				
		CL	OD	FM	RS
<i>WeakPair</i>			✓	✓	✓
<i>AeroGround</i>				✓	✓
<i>MNIST</i>		✓			

A. Dataset

WeakPair: The *WeakPair* dataset is collected in the autonomous driving simulator in four different weather conditions. It is recorded in the overhead orthomosaic perspective and is leveraged in the paper whose demonstration in different weathers is shown in Fig. 1 where S2.A is the “foggy”, S2.B is the “night”, S2.C is the “sunny”. Each task in this paper requiring this dataset has its competing methods trained with weakly-paired images to transfer adverse weathers to a sunny one in Town 1 and tests their corresponding performances in Town 2.

AeroGround: The *AeroGround* dataset is collected for aerial-ground collaboration. It contains several different image pairs shown as follows and in this paper, our experiments involving *AeroGround* are conducted on L2D and S2D:

- 1) **L2D:** “LiDAR Local Map” to “Drone’s View”;
- 2) **L2Sat:** “LiDAR Local Map” to “Satellite Map”;
- 3) **S2D:** “Stereo Local Map” to “Drone’s View”;
- 4) **S2Sat:** “Stereo Local Map” to “Satellite Map”.

Tasks requiring this dataset in the paper has their competing methods trained to transfer LiDAR representations and stereo images to the drone’s style.

MNIST: The *MNIST* dataset is a collection of hand-written numbers for the task of classification collected by [15]. We make it a weakly-paired one by changing styles via kernel disruption and Gaussian blur, and transforming poses, shown in Fig. 1(S3).

For all dataset above, we constrain translations of both x and y , rotation changes and scale changes of the two weakly-paired images in the range of $[-50, 50]$ pixels, $[0, \pi)$ and $[0.8, 1.2]$ respectively with images shapes of 256×256 .

B. Tasks and Metrics

CLASSIFICATION: Each method is trained with weakly-paired images(e.g. S3.A and S3.B in Fig. 1). We train a classifier[10] on the original S3.C and test the classification on the transferred images. We adopt average precision \mathcal{AP}_{class} and the harmonic mean of recall and \mathcal{AP}_{class} , noted as MaxF1 to evaluate the domain transfer performance.

ROAD SEGMENTATION: For the two datasets, we train the segmentation network[22] on *WeakPair*’s sunny day and on *Aero-Ground*’s drone’s perspective and test the road segmentation performance on the style transferred images. We evaluate the performance with Intersection-over-Union(IoU) \mathcal{P}_{road} (the same measurement as \mathcal{P}_{class}), and the harmony mean(MaxF1) of \mathcal{P}_{road} and \mathcal{R}_{road} .

OBJECT DETECTION: Baselines as well as PRoGAN is trained to transfer adverse weathers to a sunny one. The




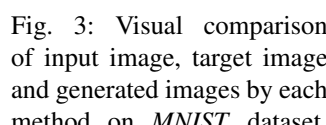
	Baselines	Classification results	
		AP	MaxF1
	Raw MNIST	93.97	94.24
	Original	64.06	57.13
	CYCLEGAN	86.71	84.20
	UGATIT	78.12	73.91
	STARGANv2	41.66	38.71
	DRIT	88.22	77.31
	MUNIT	86.97	82.08
	PIX2PIX(W)	65.43	69.68
	PIX2PIX(P)	93.22	94.01
	PRoGAN	92.58	93.88
	UGATIT		
	PIX2PIX		

Fig. 3: Visual comparison of input image, target image and generated images by each method on *MNIST* dataset. Note: 1) “Target” is the raw *MNIST* data, 2) the demonstration of PIX2PIX in the figure is the one trained on paired data.

TABLE II: Evaluation results of classification on *MNIST* dataset. PIX2PIX2(P) is claimed as PIX2PIX trained on paired data and PIX2PIX2(W) for PIX2PIX trained on weakly-paired data. AP reports the average precision and “MaxF1” reports the harmony mean.

detector[19] is trained on the sunny day and evaluates the style translation performance of each method by mean average precision (mAP) and harmony mean of precision and recall (F1).

FEATURE MATCHING: The feature matching task is carried out with SIFT[18] since it is a perfect solution to find the matching features of two images. It is adopted to evaluate the performance of each method for the more the generated data is alike with the target one, the more the SIFT points will be. We extract top 50 feature points from SIFT and calculate the true positive matching number \mathcal{N}_{SIFT} .

C. Comparative Methods

Baselines in the experiment include unpaired data based methods, CYCLEGAN[26], DRIT[16], MUNIT[11], STAR-GAN v2[3], UGATIT[14] and paired data based method PIX2PIX[12]. In classification task, all baselines above are compared, and PIX2PIX is especially involved in this task with precisely paired data. By conducting experiments on both weakly-paired data and paired-data in the *MNIST* dataset, we verify the upper bound of our method comparing to PIX2PIX in paired data and the better performance of our work comparing to rest of the baselines in weakly-paired data. For the remaining tasks, only unpaired data based methods above are compared, due to the poor performance when imperfectly aligned data is utilized.

V. EXPERIMENTS: RESULTS

A. MNIST Classification

In this experiment, we evaluate the capability bound of our approach where we assume that PRoGAN trained on weakly-paired *MNIST* should not outperform PIX2PIX trained on perfectly paired *MNIST*. While each competing method is

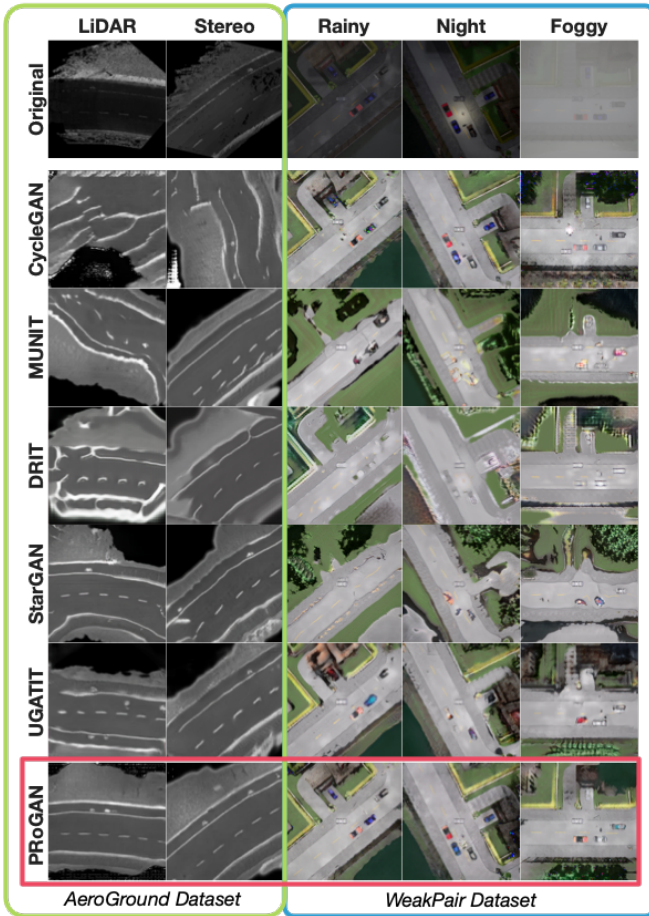


Fig. 4: Qualitative comparison of competing methods in *WeakPair* dataset and *AeroGround* dataset. The “Original” is the input of each method and the “Target” is the desired domain with weakly-paired geometrical relation. With good disentanglement, the output images of each method should only learn the style changes.

trained on weakly-paired data, baseline PIX2PIX is trained on both weakly-paired data and paired data separately. The qualitative result shown in Fig. 3 indicates that PROGAN shows the clearest result with less noise and STARGAN is unable to disentangle the two variance. The quantitative result in TABLE. II denotes that classification by [10] informs a similar quality when it is performed on the raw *MNIST* data, the output of ProGAN, and the output of PIX2PIX. It shows that PROGAN’s capability of handling weakly-paired images is almost similar to PIX2PIX ability in paired images. However, PIX2PIX trained on paired data(PIX2PIX(P)) gives the best performance while it acts terribly when being trained on weakly-paired data(PIX2PIX(W)). Therefore, we believe that PIX2PIX is no longer a suitable baseline for the following tasks as only weakly-paired data is available.

B. Road Segmentation

In this experiment, we evaluate PROGAN on the task of road segmentation in two different datasets.

WeakPair DATASET: Fig. 4 provides a qualitative comparison of the competing methods. We observe that our

TABLE III: Evaluation results of road segmentation on orthomosaic perspective in *WeakPair* dataset. The experiments is conducted on “Foggy” → “Sunny”, “Rainy” → “Sunny”, and “Night” → “Sunny”. IoU(percentage) reports the segmentation performance of roads and the higher is better.

Baselines	Foggy(IoU)		Rainy(IoU)		Night(IoU)	
	AP	MaxF1	AP	MaxF1	AP	MaxF1
Sunny(GT)	92.91	97.40	92.91	97.40	92.91	97.40
Original	65.73	77.54	23.26	37.74	30.17	37.65
CYCLEGAN	90.72	89.85	90.73	91.36	91.28	90.31
UGATIT	89.00	89.65	88.34	90.09	88.53	90.29
STARGANv2	84.06	87.15	87.86	90.35	89.82	92.15
DRIT	77.91	82.67	84.59	85.61	87.08	88.45
MUNIT	83.93	83.65	90.02	90.24	83.96	84.16
Ours(ProGAN)	92.15	94.22	93.57	96.59	92.50	96.86

TABLE IV: Evaluation results on *AeroGround* Dataset of road segmentation. The experiments is conducted both on LiDAR map → Drones’s Map and on stereo map → Drones’s Map. IoU(percentage) reports the segmentation performance of roads and the higher is better.

Baselines	S2A(IoU)		L2A(IoU)	
	AP	MaxF1	AP	MaxF1
Aerial(GT)	92.46	97.71	92.46	97.71
Original	54.67	53.59	16.12	28.26
CYCLEGAN	20.16	30.01	15.82	27.33
UGATIT	74.01	70.61	21.60	33.59
STARGANv2	74.32	77.36	12.30	20.78
DRIT	56.31	54.49	22.76	34.31
MUNIT	39.60	46.07	11.59	20.78
Ours(ProGAN)	92.06	94.09	92.10	95.21

method synthesizes images with a higher visual quality and a better disentanglement compared to the baseline models. As shown in TABLE III, our method outperforms all the baselines in terms of boosting the road segmentation in the *WeakPair* dataset. While our method is on par with the ground truth(sunny weather) in terms of performance, the CYCLEGAN, STARGAN and MUNIT is still close behind. This is due to that *WeakPair* dataset is shot from the same kind of sensors and requires less style changes other than simple changes in color and thus requires less disentanglement.

AeroGround DATASET: With the multi-agent collaborative exploration tasks involved, real-world applications are essential. Fig. 4 shows the qualitative results of each competing methods and it indicates that the competing baselines that show good performance with the simulated *WeakPair* dataset degenerate seriously in the real-world dataset where style and geometrical transformation is entangled. TABLE IV provides the corresponding quantitative comparison. The result denotes that when the style changes becomes drastic or across-sensors(e.g. from LiDAR to Aerial camera) with geometrical transform, PROGAN outperforms all these baselines by a large margin.

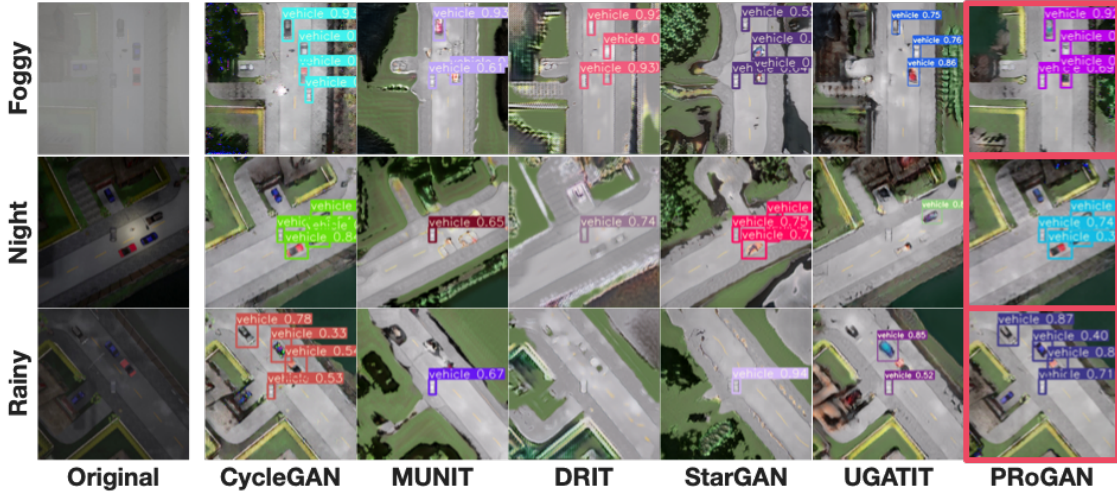


Fig. 5: Qualitative comparison of competing methods in *WeakPair* dataset and *AeroGround* dataset. The “Original” is the input of each method and the “Target” is the desired domain with weakly-paired geometrical relation.

TABLE V: Evaluation results of vehicle detection on orthomosaic perspective in *WeakPair* dataset. The experiments are conducted on “Foggy” \rightarrow “Sunny”, “Rainy” \rightarrow “Sunny”, and “Night” \rightarrow “Sunny”. “mAP(0.5)” reports the mean average precision with IOU greater than 0.5, and “F1” reports the harmonic mean of mAP(0.5) and recall.

Baselines	Foggy		Rainy		Night	
	mAP	F1	mAP	F1	mAP	F1
Sunny(GT)	92.90	92.94	92.90	92.94	92.90	92.94
Original	10.26	13.54	11.74	14.21	13.55	14.79
CYCLEGAN	53.02	59.50	49.93	49.93	56.00	55.80
UGAITIT	9.47	18.91	35.10	53.61	73.81	77.89
STARGANv2	44.55	43.06	39.52	43.33	42.00	43.84
DRIT	38.49	37.84	12.50	14.89	52.94	55.93
MUNIT	65.11	74.70	40.91	56.72	66.81	74.00
Ours(ProGAN)	86.60	87.59	88.69	90.39	88.52	89.94

C. Object Detection

Demonstration of the detection result is shown in Fig. 5. It shows that even though CYCLEGAN is able to provide images of decent quality, it tends to generate vehicles that never exist and also will inevitably generate a random shape in the center of the image. MUNIT, DRIT and STARGAN tend to neglect tiny details which results in the blurring effects in objects and thus failed to outline and paint these vehicles. Quantitative indicators shown in TABLE V show these observations above and confirms that in the aspects of retrieving details in weakly-paired and boosting object detection, PROGAN leads by a huge margin.

D. Feature Matching

We perform an aerial-ground localization in this experiment by the means of SIFT. The experiments are conducted on both the *WeakPair* dataset and *AeroGround* dataset and therefore the target image is either a “sunny day shot” or an “aerial view” respectively. TABLE VI reports the quantitative

TABLE VI: Evaluation results of boosting SIFT matching in *WeakPair* dataset and *AeroGround* dataset. We adopt \mathcal{N}_{SIFT} as the metric with the 50 as the top confidence.

Baselines	Foggy	Rainy	Night	S2A	L2A
CYCLEGAN	32.5	35.1	33.4	25.7	33.1
UGAITIT	10.9	13.3	11.2	21.5	32.8
STARGANv2	13.5	13.0	12.5	14.2	14.0
DRIT	11.3	10.9	7.5	6.0	21.9
MUNIT	29.2	39.5	11.7	23.5	28.1
Ours(ProGAN)	44.8	45.3	45.9	45.2	46.8

TABLE VII: Quantitative comparison for ablation studies on Stereo \rightarrow Aerial scene in *AeroGround* dataset. It indicates that the main contributing function is the “PRo” without whom the performance drops immediately.

Ablations	Original	w/o PRo	Basic PRoGAN	Full PRoGAN
AP	29.72	60.26	89.95	91.92
MAXF1	43.04	58.08	91.72	94.49

comparison while Fig. 6 provides a qualitative one. They indicate that our PROGAN obtains the best result on both the adverse weather scenario and the sensor alternation scenario. This experiment assures that our method can preserve more details consistently, thus resulting in more correct feature correspondences.

E. Ablation Study

Several experiments are designed for ablation studies and all of which are conducted on the *AeroGround* dataset and evaluated with the performance of road segmentation boosting. Firstly, we remove the Self-Supervised(SS) architecture(denotes as “Basic PRoGAN”) by removing the loss $\mathcal{L}_{\theta,s}$ and $\mathcal{L}_{\xi,r}$. The relevant result show in Fig. 7 indicates that the image generated without self supervision by pose estimator is a bit ambiguous in detail. Then, we further deprecate the Pose Randomization architecture (denotes as “w/o PRo”) and optimize the model by stop rotating randomly. The result

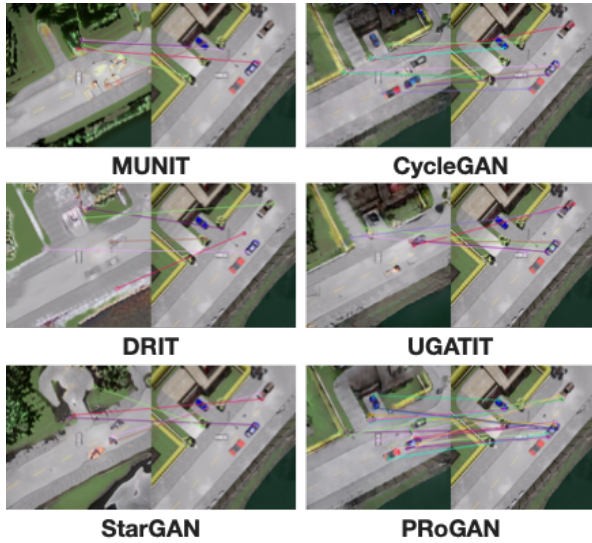


Fig. 6: Visual comparison of localization with the feature extractor of SIFT.

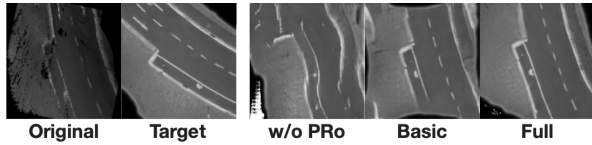


Fig. 7: Visual comparison for ablation studies on Stereo → Aerial scene in AeroGround dataset.

generated by a “w/o PPro” is totally distorted in road’s orientation and detail rehabilitation. The “w/o PPro” is tricked and misled by the highly entangled geometric transformation and fails to concentrate on style learning. The road segmentation performs weakly in all scenarios above with unsatisfying results and the quantitative comparison is shown TABLE VII. We now reassure that the Pose Randomization plays the most important roll in PProGAN while SS keeps details alive.

VI. CONCLUSION

We present an approach for style translation between weakly-paired images who are entangled in style and pose transformations. To achieve this, we disentangle the style and pose with pose randomization and train a GAN network with self-supervision by differentiable pose estimator, namely PProGAN. In various experiments, the proposed PProGAN presents the better performances than other comparative methods, showing its potential for real application.

REFERENCES

- [1] Ting Chen et al. “Self-supervised gans via auxiliary rotation loss”. In: *Proceedings of the IEEE Conference on Computer Vision and Pattern Recognition*. 2019.
- [2] Zexi Chen et al. “Deep Phase Correlation for End-to-End Heterogeneous Sensor Measurements Matching”. In: *arXiv preprint arXiv:2008.09474* (2020).
- [3] Yunjey Choi et al. “Stargan v2: Diverse image synthesis for multiple domains”. In: *Proceedings of the IEEE/CVF Conference on Computer Vision and Pattern Recognition*.
- [4] Yunjey Choi et al. “StarGAN: Unified Generative Adversarial Networks for Multi-Domain Image-to-Image Translation”. In: *Proceedings of the IEEE Conference on Computer Vision and Pattern Recognition*. 2018.
- [5] Jeff Donahue and Karen Simonyan. “Large Scale Adversarial Representation Learning”. In: *Advances in Neural Information Processing Systems* 32. Curran Associates, Inc., 2019.
- [6] Alexey Dosovitskiy et al. “CARLA: An Open Urban Driving Simulator”. In: *Conference on Robot Learning*. 2017.
- [7] Alberto Garcia-Garcia et al. “A survey on deep learning techniques for image and video semantic segmentation”. In: *Applied Soft Computing* 70 (2018).
- [8] Spyros Gidaris, Praveer Singh, and Nikos Komodakis. “Unsupervised representation learning by predicting image rotations”. In: *arXiv preprint arXiv:1803.07728* (2018).
- [9] Ian Goodfellow et al. “Generative adversarial nets”. In: *Advances in neural information processing systems*. 2014.
- [10] Kaiming He et al. “Deep residual learning for image recognition”. In: *Proceedings of the IEEE conference on computer vision and pattern recognition*. 2016.
- [11] Xun Huang et al. “Multimodal Unsupervised Image-to-image Translation”. In: *ECCV*. 2018.
- [12] Phillip Isola et al. “Image-to-Image Translation with Conditional Adversarial Networks”. In: *CVPR* (2017).
- [13] Justin Johnson, Alexandre Alahi, and Li Fei-Fei. “Perceptual losses for real-time style transfer and super-resolution”. In: *European conference on computer vision*. Springer. 2016.
- [14] Junho Kim et al. “U-gat-it: unsupervised generative attentional networks with adaptive layer-instance normalization for image-to-image translation”. In: (2019).
- [15] Yann LeCun et al. “Gradient-based learning applied to document recognition”. In: *Proceedings of the IEEE* (1998).
- [16] Hsin-Ying Lee et al. “DRIT++: Diverse Image-to-Image Translation via Disentangled Representations”. In: *International Journal of Computer Vision* (2020).
- [17] Ming-Yu Liu, Thomas Breuel, and Jan Kautz. “Unsupervised image-to-image translation networks”. In: *Advances in neural information processing systems*. 2017, pp. 700–708.
- [18] David G Lowe. “Distinctive image features from scale-invariant keypoints”. In: *International journal of computer vision* 60.2 (2004), pp. 91–110.
- [19] Joseph Redmon and Ali Farhadi. “Yolov3: An incremental improvement”. In: *arXiv preprint arXiv:1804.02767* (2018).
- [20] Zehang Sun, George Bebis, and Ronald Miller. “On-road vehicle detection: A review”. In: *IEEE transactions on pattern analysis and machine intelligence* 28.5 (2006), pp. 694–711.
- [21] Li Tang et al. “Adversarial Feature Disentanglement for Place Recognition Across Changing Appearance”. In: *2020 IEEE International Conference on Robotics and Automation (ICRA)*. IEEE. 2020, pp. 1301–1307.
- [22] Marvin Teichmann et al. “Multinet: Real-time joint semantic reasoning for autonomous driving”. In: *2018 IEEE Intelligent Vehicles Symposium (IV)*. IEEE. 2018, pp. 1013–1020.
- [23] Josh Tobin et al. “Domain randomization for transferring deep neural networks from simulation to the real world”. In: *2017 IEEE/RSJ International Conference on Intelligent Robots and Systems (IROS)*. IEEE. 2017, pp. 23–30.
- [24] Ngoc-Trung Tran et al. “An Improved Self-supervised GAN via Adversarial Training”. In: *arXiv preprint arXiv:1905.05469* (2019).
- [25] Xiangyu Yue et al. “Domain randomization and pyramid consistency: Simulation-to-real generalization without accessing target domain data”. In: *Proceedings of the IEEE International Conference on Computer Vision*. 2019, pp. 2100–2110.
- [26] Jun-Yan Zhu et al. “Unpaired Image-to-Image Translation using Cycle-Consistent Adversarial Networks”. In: *Computer Vision (ICCV)*. 2017.
- [27] ZJU-Lab. *WeakPair Dataset*. 2020. URL: <https://github.com/ZJU-Robotics-Lab/OpenDataSet>.